A KERNEL APPROACH TO COMPRESSED SENSING PARALLEL MRI

Yuchou Chang[1], Kevin F. King[2], Dong Liang[3], Yong Wang[1,4], Leslie Ying[1]

[1]Department of Electrical Engineering and Computer Science, University of Wisconsin-Milwaukee, Milwaukee, WI, USA
[2]Global Applied Science Laboratory, GE Healthcare, Waukesha, WI, USA
[3]Shenzhen Institutes of Advanced Technology, Chinese Academy of Sciences, Shenzhen, P.R. China
[4]School of Electronic Engineering, Xidian University, Xi'an, P.R. China

ABSTRACT

Compressed sensing (CS) and parallel imaging (PI) have been widely studied for accelerating MRI reconstruction. Furthermore, the serial combination methods of CS and PI have been proposed for even higher speed of reconstruction. However, both reconstructed signals by CS and PI are not as accurate as acquired MR signals, so that errors of CS reconstruction as the first step will be propagated and even amplified to deteriorate PI reconstruction quality in the second step. Based on our previous work – nonlinear GRAPPA (NLGRAPPA), we proposed a novel serial combination of CS and NLGRAPPA (CS-NLGRAPPA) reconstruction. The generalized kernel regression model of NLGRAPPA can remove error effects of inaccurate signal reconstruction by CS. Experimental results using phantom and *in vivo* data demonstrate that the proposed CS-NLGRAPPA method can significantly improve the reconstruction quality over the existing method and push net reduction factor around 4.

Index Terms— Parallel MRI, GRAPPA, Compressed Sensing, Kernel Method, Nonlinear GRAPPA

1. INTRODUCTION

MR imaging speed is usually limited by the large number of samples needed along the phase encoding direction. In conventional MRI using Fourier encoding, the required number of samples is determined by the field of view and the resolution of the image based on the Shannon sampling theory. To accelerate conventional MRI, both parallel imaging (pMRI) and compressed sensing (CS) have been used to reduce the number of acquired data. In pMRI, due to the availability of multi-channel coils, the MR images can be reconstructed from multi-channel *k*-space data sampled below the Nyquist sampling rate using reconstruction methods such as SENSE [1] and GRAPPA [2]. Theoretically, the maximum reduction factor can be up to the number of channels under ideal conditions. However, this maximum usually cannot be achieved due to practical limitations such as noise and imperfect coil geometry. CS MRI [3] is based on CS theory [4,5], a new framework for data sampling and signal recovery. CS-MRI takes advantage of the fact that MRI meets two conditions of CS. One is the MR images are sparse or compressible after certain transformations. The other is the Fourier encoding is incoherent with these sparse transformations. Therefore, the MR images can be reconstructed using a nonlinear convex program from data sampled at a rate close to their intrinsic information rate which is well below the Nyquist rate.

Because pMRI and CS reduce sampling based on complementary information, several methods [6-9] have been developed to combine pMRI and CS for further reduction. Among these methods, the ones that sequentially carry out CS reconstruction for the aliased image of each channel and parallel imaging for the final unfolded image have demonstrated several advantages [7,8]. First, because the CS and pMRI procedures are clearly decoupled, any CS or pMRI methods are directly applicable without modifications. Second, the sampling pattern can be designed to satisfy different requirements for CS and pMRI. Finally, the acceleration factor of the combined approach is a product of the factors achieved by CS and pMRI individually.

However, an issue with the sequential method is error propagation. The error in CS reconstruction may propagate and be amplified in the pMRI step according to the g-factor. For example in CS-SENSE [7], SENSE with inaccurate coil sensitivities accentuates the CS reconstruction error. In CS-GRAPPA [8], the g-factor of GRAPPA increases dramatically with the acceleration factors and thus magnifies the CS error. We have recently developed a nonlinear GRAPPA (NLGRAPPA) method [10] using kernel method. The method has shown to reduce the g-factor significantly at high acceleration factors.

In this paper, we propose a novel sequential approach that performs CS followed by nonlinear GRAPPA. The proposed method, named CS-NLGRAPPA, first employs CS to reconstruct a set of multi-channel aliased images (i.e., *k*-space data on a uniformly undersampled grid in each channel), and then applies NLGRAPPA to reconstruct the missing *k*-space data for the final root sum-of-squares (SOS) reconstruction. Due to the nonlinear characterization ability

in the generalized regression model, the kernel method can remove error effects generated by CS reconstruction to certain extent. Experimental results demonstrate that the proposed method outperforms CS-GRAPPA in suppressing the spatial-varying noise and aliasing artifacts with high accelerations.

2. PROPOSED METHOD

2.1 Sampling pattern

The sampling pattern for the proposed method has two parts. The first part is the same as the sampling used in CS-SENSE [7]. Specifically, a variable-density random sampling scheme [3] is employed to further undersample the data along the phase encoding direction that is already undersampled in pMRI, as shown in Figure 1 from (a) to (b), where the white lines represent the uniformly undersampled *k*-space locations, while black regions denote the unacquired locations. The other part acquires the fully sampled auto-calibration signal (ACS) at the central *k*-space. Because the variable-density sampling usually acquires the central *k*-space in full as well, the two parts have many overlapping lines. The union of the randomly undersampled *k*-space lines (Figure 1 (b)) and the auto-calibration signal (ACS) lines (Figure 1 (c)) produces the ultimate sampling pattern as shown in figure 1 (e) for the proposed method. The net reduction factor is calculated by the total number of acquired lines divided by the number of lines when full sampling is employed. As we can see, the net reduction factor for the proposed method in Figure 1 (e) is higher than that for conventional GRAPPA which uses the sampling in Figure 1 (d).

2.2. Sequential reconstruction

The proposed method carries out CS and NLGRAPPA reconstructions sequentially. In the CS step, the uniformly undersampled data are reconstructed from the randomly undersampled data as shown in Figure 1 from (b) to (a). To this end, CS is used to reconstruct the aliased image in each channel and then Fourier transformed to obtain the uniformly undersampled *k*-space data. If $\mathbf{f}_l^A$ is a vector for the aliased reduced FOV image from the *l*-th channel, the data consistence comes from

$$\mathbf{F}^u \mathbf{f}_l^A = \mathbf{d}_l^u \tag{1}$$

where $\mathbf{F}^u$ represents Fourier encoding operation and $\mathbf{d}_l^u$ is the undersampled *k*-space data from *l*-th channel. Therefore, the aliased image $\mathbf{f}_l^A$ at each channel can be reconstructed using CS

$$\arg\min_{\mathbf{f}_l^A} \left\{ \left\| \mathbf{F}^u \mathbf{f}_l^A - \mathbf{d}_l^u \right\|_2^2 + \lambda_1 \left\| \boldsymbol{\psi} \mathbf{f}_l^A \right\|_1 + \lambda_2 \mathrm{TV}\left(\mathbf{f}_l^A\right) \right\} \tag{2}$$

where $\boldsymbol{\psi}$ adopts wavelet transform and TV represents total variation.

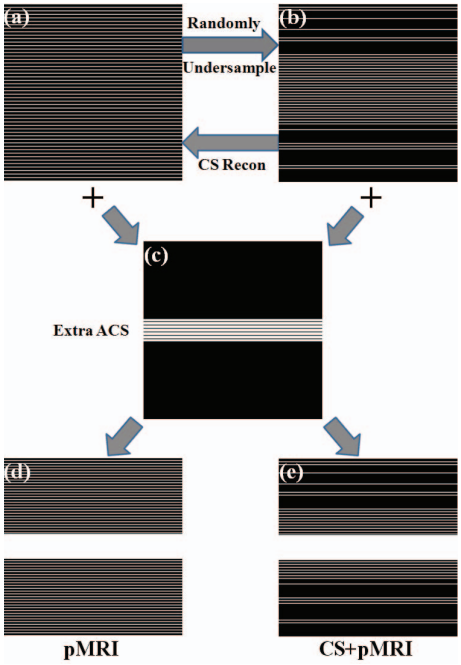


Fig. 1 Sampling pattern and CS reconstruction demonstration of the proposed method.

In the NLGRAPPA steps, the ACS data in Figure 1 (c) are used for calibration and the uniformly undersampled data in Figure 1 (a) obtained from the CS step are used for reconstruction of the final image. NLGRAPPA is used for calibration and reconstruction. The method has shown to suppress the nonlinear error in GRAPPA due to the errors-in-variables problem. In NLGRAPPA, a generalized, nonlinear model is exploited to characterize the relationship between the acquired data and missing data. Kernel method is used to represent the nonlinear relationship such that the linear least squares algorithm is still applicable for the underlying nonlinear problem. Specifically, NLGRAPPA transforms original input space (original *k*-space here) to a high dimensional feature space using a nonlinear mapping. A polynomial kernel is used here so that the acquired *k*-space data are nonlinearly mapped using a truncated second-order polynomial function. The unacquired *k*-space signal S_j is obtained by a nonlinear combination of the acquired *k*-space signals S_l:

$$\begin{aligned} S_j\left(k_y + r\Delta k_y, k_x\right) = {} & w_{j,r}^{(0)} \times 1 + \sum_{l=1}^{L}\sum_{b=B_1}^{B_2}\sum_{h=H_1}^{H_2} w_{j,r}^{(1)}(l,b,h) \times S_l\left(k_y + bR\Delta k_y, k_x + h\Delta k_x\right) \\ & + \sum_{l=1}^{L}\sum_{b=B_1}^{B_2}\sum_{h=H_1}^{H_2} w_{j,r}^{(2,0)}(l,b,h) \times S_l^2\left(k_y + bR\Delta k_y, k_x + h\Delta k_x\right) \\ & + \sum_{l=1}^{L}\sum_{b=B_1}^{B_2}\sum_{h=H_1}^{H_2-1} w_{j,r}^{(2,1)}(l,b,h) \times S_l\left(k_y + bR\Delta k_y, k_x + h\Delta k_x\right) \times \\ & \quad S_l\left(k_y + bR\Delta k_y, k_x + (h+1)\Delta k_x\right) \\ & + \sum_{l=1}^{L}\sum_{b=B_1}^{B_2}\sum_{h=H_1}^{H_2-2} w_{j,r}^{(2,2)}(l,b,h) \times S_l\left(k_y + bR\Delta k_y, k_x + h\Delta k_x\right) \times \\ & \quad S_l\left(k_y + bR\Delta k_y, k_x + (h+2)\Delta k_x\right) \end{aligned} \tag{3}$$

where w denotes the coefficient set, R represents the outer reduction factor, j is the target coil, l counts all coils, b and h transverse the acquired neighboring k-space data in k_y and k_x directions respectively, and the variables k_x and k_y represent the coordinates along the frequency- and phase-encoding directions, respectively. The nonlinear formulation of Eq. [3] represents a more general model for GRAPPA, which includes the conventional GRAPPA as a special case. It is seen that the first-order terms of nonlinear GRAPPA is equivalent to the conventional GRAPPA, which mainly captures the linear relationship between the missing and acquired undersampled data in the absence of noise and approximations. The second-order terms of Eq. [3] can be used to characterize other nonlinear effects in practice such that noise and approximation errors are suppressed in reconstruction. The proposed formulation is a nonlinear model in the sense that nonlinear combination of acquired data contributes to estimation of missing k-space data.

Under such a mapping, we still only need to solve the following linear system equation in the feature space:

$$\mathbf{b} = \Phi(\mathbf{A})\mathbf{x} \,, \tag{4}$$

where x represents the reconstruction coefficients, $\Phi(\mathbf{A})$ is a matrix representing the nonlinear mapping. It is seen that the calibration process to find $\mathbf{x}$ can still be easily and linearly solved in the high dimensional feature space by a linear algorithm:

$$\hat{\mathbf{x}} = \left(\left(\Phi(\mathbf{A}) \right)^H \left(\Phi(\mathbf{A}) \right) \right)^{-1} \left(\Phi(\mathbf{A}) \right)^H \mathbf{b} \,, \tag{5}$$

although the relationship between the acquired and missing k-space data is nonlinear. Other linear computational algorithms such as reweighted least-squares and total least-squares methods can also be used here. Once the coefficients are estimated in Eq. (5), they are plugged back in Eq. (4) to reconstruct the missing data in outer k-space, like the conventional GRAPPA does.

4. EXPERIMENTAL RESULTS

The proposed method was tested on both phantom and *in vivo* data sets. An 8-channel phantom dataset was acquired using a Gradient Echo sequence (TE/TR = 10/100 ms, 31.25 kHz bandwidth, matrix size = 256×256, FOV = 250 mm^2). An 8-channel brain dataset was obtained using a 2D spin echo (SE) sequence (TE/TR = 11/700 ms, matrix size = 256 × 256, FOV = 220 mm^2). A set of cardiac cine images was acquired using a 2D trueFISP sequence (TE/TR=1.67/50.1 ms, bandwidth 903 Hz/pixel, 45 degree flip angle, 8mm slice thickness, 34 cm FOV in readout direction, 256x146 acquisition matrix) with a 12-channel cardiac coil but combined to 4 channels. All data sets were acquired in full and then manually undersampled to simulate the accelerated acquisition. The sum-of-squares (SoS) reconstruction from the fully sampled data of all channels was used as the reference image for comparison. The reconstructions from reduced data using the CS-GRAPPA and the proposed CS-NLGRAPPA method were compared. In both methods, the number of blocks (size of b) is 2 and the number of columns (size of h) is 15 for all datasets. For the eight-channel phantom data, a net reduction factor of 4 was achieved by a combination of 1.5 for CS and outer reduction factor (ORF) = 6 with 42 ACS for GRAPPA/NLGRAPPA. For the eight-channel brain data, the net reduction factor is 3.93 with CS 1.7, ORF = 4, and ACS = 36. In the four-channel cardiac experiment, the net reduction factor is 4.12 with CS 2.0, ORF = 4, and 40 ACS lines.

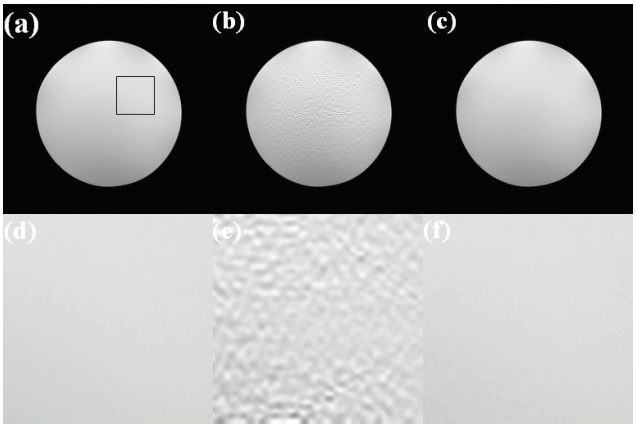


Fig. 2 With (a) the SoS reconstruction of the 8-chanel phantom image as the reference, we compare (b) CS-GRAPPA and (c) the proposed method at a net reduction factor of 4. Subfigures (d) – (f) show zoomed-in regions of (a) – (c) respectively.

Figure 2 shows the reconstructions of the phantom. A small region is zoomed to show more details. It is seen that the CS-GRAPPA suffers from large noise and aliasing artifacts at a net reduction factor of 4.00. The proposed CS-NLGRAPPA method can suppress both noise and artifacts at such a high acceleration.

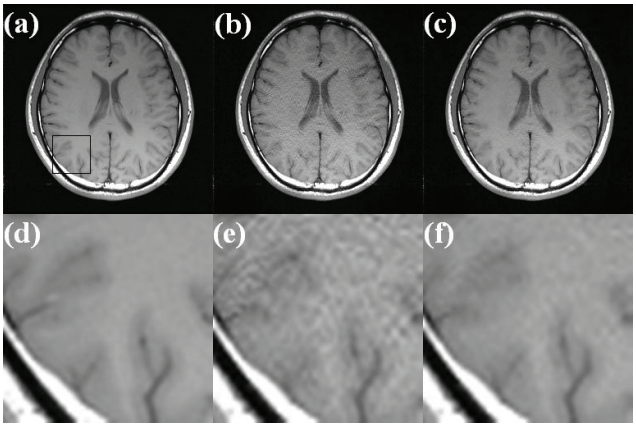


Fig. 3 With (a) the SoS reconstruction of the 8-chanel brain image as the reference, we compare (b) CS-GRAPPA and (c) the proposed method at a net reduction factor of 3.93.

Figure 3 shows the reconstruction results from a set of *in vivo* brain data. As shown in the zoomed regions, the

proposed method not only effectively removes the spatial-varying noise and aliasing artifacts in the CS-GRAPPA reconstruction, but also preserves details well without blurring boundaries. The CS-NLGRAPPA can push the net reduction factor to 3.93.

The reconstruction results of the cardiac dataset are presented in Fig. 4. In contrast to the CS-GRAPPA reconstruction, the reconstruction by the proposed method is much cleaner with a slight loss of resolution at a high net reduction factor of 4.12.

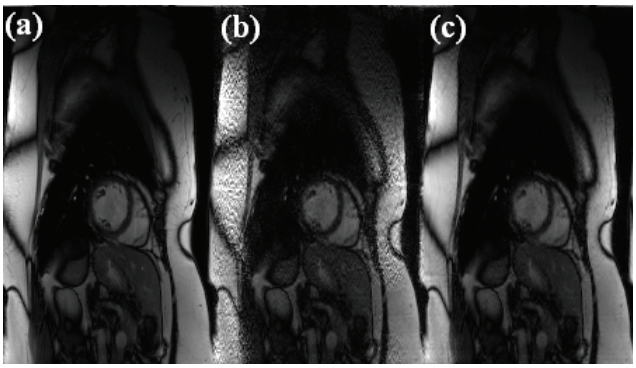


Fig. 4 Comparison of (a) SoS, (b) CS-GRAPPA and (c) the proposed method in reconstructing the four-chanel cardiac image at a net reduction of 4.12.

The computational time of both methods is compared in Table 1. The proposed method takes about 1.7 - 2 times of CS-GRAPPA for reconstruction.

Table 1 Comparision of computational time

	Phantom	Brain	Cardiac
CS-GRAPPA	208 s	140 s	67 s
CS-NLGRAPPA	429 s	267 s	116 s

We investigate how different numbers are to be distributed among the CS, ORF and ACS to achieve the optimal quality at a fixed net reduction factor. It is known that high accelerations in CS can lead to aliasing artifacts and loss of resolution. On the other hand, high ORFs usually deteriorate SNR and require more ACS to avoid aliasing. The study was carried out on the eight-channel brain dataset. The results are shown in Fig. 5. For a fixed net reduction factor of 3.93 and ORF of 4 for the NLGRAPPA step, we tested on three different combinations of ACS and reduction for CS (R_{CS}). When 26 ACS lines and R_{CS} = 1.4 were used, aliasing artifacts appear due to insufficient number of ACS lines. The appearance of artifacts is in form of folding that is typical of parallel imaging. When 44 ACS lines and R_{CS} = 2.0 were used, aliasing artifacts appear due to propagation of CS reconstruction error. The appearance is rather incoherent due to the random sampling. The intermediate combination of 36 ACS and R_{CS} = 1.7 generates the optimal reconstruction for this dataset. In general, the reduction in CS cannot be high due to error propagation. A factor of lower than 2 is usually used.

5. CONCLUSION

In this paper, we propose a novel method that combines CS with nonlinear GRAPPA sequentially for fast imaging. NLGRAPPA is applied on the *k*-space data reconstructed by CS. The experimental results demonstrate that the proposed CS-NLGRAPPA method is superior to CS-GRAPPA in suppressing both noise and artifacts when a high net reduction factor is used.

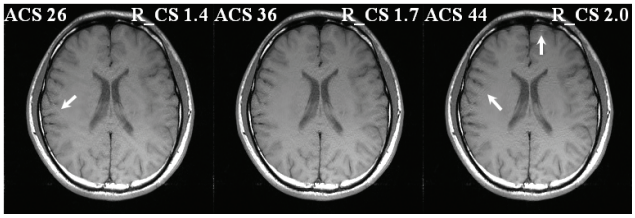


Fig. 5 CS-NLGRAPPA reconstructions with three different combinations of ACS and R_{CS} with fixe ORF of 4 and a net reduction factor of 3.93.

6. ACKNOWLEDGMENT

This work was supported in part by the National Science Foundation CBET-0731226.

7. REFERENCES

[1] K.P. Pruessmann, M. Weiger, M.B. Scheidegger, and P. Boesiger, "SENSE: Sensitivity encoding for fast MRI," *Magn. Reson. Med.*, vol. 42, pp. 952-962, Nov. 1999.

[2] M.A. Griswold, P.M. Jakob, R.M. Heidemann, N. Mathias, V. Jellus, J. Wang, B. Kiefer, and A. Haase, "Generalized autocalibrating partially parallel acquisitions (GRAPPA)," *Magn. Reson. Med.*, vol. 47, pp. 1202-1210, Jun. 2002.

[3] M. Lustig, D. Donoho, and J.M. Pauly, "Sparse MRI: The application of compressed sensing for rapid MR imaging," *Magn. Reson. Med.*, vol. 58, pp. 1182-1195, Dec. 2007.

[4] E. J. Candès, J. Romberg, and T. Tao, "Robust uncertainty principles: Exact signal reconstruction from highly incomplete frequency information," *IEEE Trans. Inf. The.*, vol. 52, pp. 489-509, Feb. 2006.

[5] D. Donoho, "Compressed sensing," *IEEE Trans. Inf. The.*, vol. 52, pp. 1289 - 1306, Apr. 2006.

[6] B. Liu, F. Sebert, Y. M. Zou, and L. Ying, "SparseSENSE: application of compressed sensing in parallel MRI", In *Proc. of 16th ISMRM Scientific Meeting*, (Toronto, Canada), 3154, May 2008.

[7] D. Liang, B. Liu, J. Wang, and L. Ying, "Accelerating SENSE using compressed sensing," *Magn. Reson. Med.*, vol. 62, pp. 1574-1584, Dec. 2009.

[8] K. Kevin, D. Xu, A. C. Brau, P. Lai, P. J. Beatty, and L. Marinelli, "A new combination of compressed sensing and data driven parallel imaging," In *Proc. of 18th ISMRM Scientific Meeting*, (Stockholm, Sweden), 4881, May 2010.

[9] M. Lustig, and J.M. Pauly, "SPIRiT: iterative self-consistent parallel imaging reconstruction from arbitrary *k*-space," *Magn. Reson. Med.*, vol. 64, pp. 457-471, Aug. 2010.

[10] Y. Chang, D. Liang, and L. Ying, "Nonlinear GRAPPA: a kernel approach to parallel MRI reconstruction," *Magn. Reson. Med.* in print, 2011.